Energy Proceedings
Vol 30, 2023
ISSN 2004-2965

Study of the combustion performance of new biomass heating stoves

Zhijie Zhang[1], Yanqiang[1*] Di, Chen Zhao[1], Zhen Li[2], Shousong Liu[1], Haiyan Di[1], Mengying Li[1]

1 China Academy of Building Research, Beijing, 100013, China

2 Inner Mongolia University of Science & Technology, Baotou, 014000, China

ABSTRACT

This paper investigates the combustion performance of a new biomass heating stove. Firstly, a typical structure of a house is used as the design object for load calculation; then the stove structure is designed for experimental system design, and the results of the simulation and experiment are compared with the corresponding working conditions to test the model, and the model is used to analyze the factors influencing the pellet accumulation resistance, and the influence law of the pellet parameters on the accumulation resistance is obtained. The combustion characteristics of biomass pellets are investigated and combined with static stacking characteristics and dynamic combustion characteristics, firstly, a combustion model is established and the size range of feasible biomass pellets is initially determined by measuring the combustion efficiency in terms of the percentage of volatilization analysis during the pellet combustion process; subsequently, the volatilization analysis cloud at the central interface of the stove is changed and the morphological parameters of the pellets in the model are changed to obtain the influence of the size change of the pellets in this range on the volatilization The effect of the change in particle size on the volatilization of the particles in this range is then obtained.

Keywords: biomass fuels, heating stoves, combustion simulation, resistance simulation, combustion characteristics

1. INTRODUCTION

In most of the rural areas in northern China, winter heating has long been dominated by the burning of loose coal due to the lack of centralized village distribution, poor infrastructure conditions and the high cost of centralized heating. However, under the existing conditions in rural areas, coal is not burned sufficiently and the energy utilization rate is low, which not only has poor heating effect and dirty environmental hygiene, but also leads to serious indoor air pollution [1-2], Completion of threats to the health of personnel [3-4], A large number of non-renewable resources are also being consumed day by day. The development and use of new clean energy to solve the winter heating problem in rural areas has become an important livelihood project of great interest and concern to the whole society.

Matter-forming fuels are solid fuels with a regular shape made from straw, corn cobs and dead branches of trees as the main raw material and processed mechanically. Like straw, they mainly consist of three aggregates of cellulose, hemicellulose and lignin. Some scholars have extended the Ergun equation to resistance studies of non-spherical pellet accumulation beds by using the equivalent diameter method and re-giving the values of the Ergun constant [5-10]. Atmakidi and Kenig [11] by CFD simulations to investigate the effect of confining walls on pressure drop in a medium diameter ratio particle filled bed.

Niksa [12] by comparing burn-up times with particle mass and size, it was found that a reduction in particle size or an increase in the length-to-diameter ratio would weaken convective heat transfer and lead to a longer burn-up time for volatile fraction. Panahi [13] By comparing the porosity of the remaining charcoal balls after volatile analysis out of different materials and different diameters of particles, it is found that the small initial diameter leads to the generation of thin-walled charcoal particles with small porosity which is not conducive to the final particle combustion. The combustion stage is divided into two main types of material combustion, precipitation of gaseous volatile fraction and the surrounding high temperature air mixed together quickly in the furnace chamber to complete combustion, combustion is complete in the case of the main generation of carbon dioxide and water, releasing a large amount of heat; the fuel on the grate after volatile analysis out into coke, after a series of reactions to generate carbon monoxide and hydrogen, and constantly produce ash, carbon monoxide and hydrogen in the furnace chamber The main factors affecting combustion include the heat content, water content and

geometry of the biomass forming fuel, as well as the combustion temperature.

2. DESIGN

2.1 Load calculation

In this paper, a house with a typical structure in the northern countryside is used as the design object to calculate the winter heat load of the building in the cold region of Harbin and the cold region of Beijing respectively, so as to lay the foundation for the design of the stove. The thermal parameters of the envelope structure are based on JGJ26-2018 Energy Efficiency Design Standards for Residential Buildings in Severe Cold and Cold Regions [14], The values of the relevant parameters are shown in Table 1.

Table 1. Thermal performance parameters of the external envelope

Enclosure parameters	location	
	Harbin	***Beijing***
Heat transfer coefficient of external walls [W/(m²·K)]	0.25	0.35
Heat transfer coefficient of external Windows [W/(m²·K)]	1.4	1.8
Roof heat transfer coefficient [W/(m²·K)]	0.15	0.25
Thermal resistance of the surrounding ground insulation layer (m²·K/W)	2.00	1.60

2.2 Stove design

Combustion calculations mainly include the calculation of the amount of air required for combustion and the amount of flue gas generated by combustion, both of which are based on the elemental composition and stoichiometric equation of the fuel, with straw as the main raw material for biomass forming fuel in China. The amount of air required for the complete combustion of the various combustible elements in the fuel is known as the theoretical air volume and is calculated in the following formula. In order to make the fuel burn as completely as possible in the furnace, the total air excess coefficient α is taken as 1.5 and allocated by a primary air excess coefficient of 0.8 and a secondary air excess coefficient of 0.7.

$$V^0 = 0.0899(C_{ar} + 0.375S_{ar}) + 0.265H_{ar} - 0.0333O_{ar}$$

In which V^0-the theoretical amount of air required for combustion (Nm^3/kg);

C_{ar}-mass per cent content of carbon in the fuel (%);

S_{ar}-mass per cent content of sulphur in the fuel (%);

H_{ar}-mass per cent content of hydrogen in the fuel (%);

O_{ar}-mass percentage content of oxygen in the fuel (%).

The amount of air supplied is equal to the theoretical amount of air, and the amount of flue gas produced when the fuel reaches a state of complete combustion becomes the theoretical amount of flue gas, but the actual amount of flue gas during combustion includes the amount of excess air and the amount of water vapor carried by the air.

$$V_{RO_2}^0 = 1.866\frac{C_{ar}}{100} + 0.7\frac{S_{ar}}{100}$$

$$V_{N_2}^0 = 0.8\frac{N_{ar}}{100} + 0.79V^0$$

$$V_{H_2O}^0 = 11.1\frac{H_{ar}}{100} + 1.24\frac{M_{ar}}{100} + 0.0161V^0$$

$$V_y^0 = V_{RO_2}^0 + V_{N_2}^0 + V_{H_2O}^0$$

$$V_y^0 = V_{RO_2}^0 + V_{N_2}^0 + V_{H_2O}^0$$

In which $V_{RO_2}^0$ -the sum of the volumes of carbon dioxide and sulphur dioxide in the flue gas (Nm^3/kg);

$V_{N_2}^0$ -the volume of nitrogen in the flue gas (Nm^3/kg);

N_{ar}-the mass percentage content of nitrogen in the fuel (%);

$V_{H_2O}^0$ -volume of water vapor in the flue gas (Nm^3/kg);

M_{ar}-mass per cent content of water in the fuel (%);

V_y^0 -theoretical flue gas volume (Nm^3/kg);

V_y-actual flue gas volume (Nm^3/kg);

α——excess air coefficient.

Based on the heat load and the thermal efficiency of the stove, the fuel consumption is calculated.

$$B = \frac{qt}{\eta Q_{net}}$$

In which B-fuel consumption (kg/h);

q-heat load (W);

t-length of heating time (s);

η-thermal efficiency of the stove (%);

Q_{net}-low level heat output of the fuel (kJ/kg).

The range of heat load taking values was determined in combination with the heat load per unit area in the previous section, with the lowest being the heat load of a building with a heating area of 100 m2 located in rural Beijing and the highest being the heat load of a building with a heating area of 192 m2 located in rural Harbin. The final calculation results are summarized in Table 2.

Table 2. Combustion calculation results

Location	Load index (W/m^2)	Total heat load (W)	Fuel quantity (kg/h)	Primary air volume (m^3/h)	Secondary air volume (m^3/h)	Flue gas volume (m^3/h)
Harbin	56.9	10911	10.2	32.2	28.2	60.1
Beijing	38.4	3840	3.6	11.4	9.9	21.2

2.3 Stove structure

Refer to the literature for biomass forming fuel household stoves [15-18] The structure of the furnace

chamber is shown in Figure 1. The biomass forming fuel is poured in from the furnace lid and forms a pile on the grate, which is burned under the action of primary air to produce combustible gas, which rises and mixes with secondary air to further burn fully.

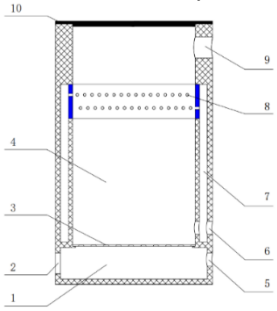

1. ash hopper 2. ash outlet 3. grate 4. furnace chamber 5. primary air outlet 6. secondary air outlet 7. secondary air duct 8. secondary air distribution ring 9. smoke exhaust 10. furnace cover

Figure 1. Schematic diagram of furnace structure

3. EXPERIMENT AND SIMULATION

3.1 Experimental system design

The experimental system design includes: selecting the nozzle according to the air volume measurement range, designing the nozzle box with the size of the selected nozzle, calculating the resistance value of the system under the maximum air volume and selecting the appropriate fan. Table 2 shows that the air volume range of 11.4m^3/h-32.2m^3/h, in order to meet the test requirements, this paper uses the throat diameter of 10mm, 15mm, 20mm nozzle according to Table 3, respectively, the measured air volume range of 4.2m^3/h-40m^3/h.

Table 3. Nozzle Selection reference table

Throat diameter(mm)	Lower measurement limit(m^3/h)	Measurement upper limit(m^3/h)	Throat diameter(mm)
8	2.7	6.3	8
10	4.2	9.9	10
15	9.5	22.3	15
20	17.0	40.0	20
25	26.5	61.8	25

nozzle box design with reference to the GB/T 17758-2010 unitary air conditioner standards in the relevant provisions of the experiment using three nozzle diameters were 10mm, 15mm, 20mm, the design of the nozzle centerline and the distance between the wind chamber wall 35.4mm, before and after the static pressure measurement point from the nozzle section distance are 32mm, the nozzle section before and after the placement of the orifice plate of 18mm diameter is used to equalize the flow.

The total resistance includes along-range resistance and local resistance, both are closely related to the flow velocity, so we need to determine the diameter of the pipe according to the approximate flow velocity (3m/s-5m/s), and then find out the actual flow velocity according to the pipe diameter, and finally bring the actual flow velocity into the resistance calculation formula to get the resistance value, and determine the pressure value required for the primary side fan and secondary side fan respectively.

3.2 Experimental methods and materials

The stacked pellets were all pine processed into cylindrical biomass pellet fuel, of which 5.11kg were pellets with diameter 6mm L/D ratio 3 and 4.27kg were pellets with diameter 6mm L/D ratio 4, i.e., both were randomly and loosely stacked in the designed stove according to the mass ratio of 1.2:1, and the stacking process was shown in Figure 2.

Figure 2. Fuel pellet pile

3.3 Experimental results and analysis

The experimental environment temperature 25.9℃, humidity 65.5%, atmospheric pressure 100.5 kPa. the data recorded for the stacking resistance experiments are shown in Table 4, where the number of the static pressure ring attached to the furnace, in increasing order from bottom to top. From the table can be seen: nozzle before the static pressure and nozzle before and after the differential pressure value is not much difference, indicating that most of the pressure head provided by the fan are lost at the nozzle, nozzle after the resistance of other parts and pipes are very small; when the air volume increases, the differential pressure between the static pressure ring increases; because the air through the grate into the furnace chamber, it takes a certain flow length to develop into a stable flow state, so calculate the resistance per unit length of the stacking section The differential pressure data between 2-3 is chosen.

Table 4. Resistance test data

Air volume (m^3/h)	Differential pressure between front and rear of nozzle (Pa)	Nozzle front static pressure (Pa)	1-2 Differential pressure between (Pa)	1-3 Differential pressure between (Pa)	2-3 Differential pressure between (Pa)
18.50	160.5	161.5	0.3	0.4	0.1
21.58	217.5	219.5	0.5	0.7	0.2
24.67	285.0	286.4	0.6	0.8	0.2
30.21	426.6	429.3	0.8	1.1	0.3
30.83	445.5	448.7	0.8	1.1	0.3

3.4 CFD-based drag simulation

Unlike previous treatments such as reducing the particle size [19] and increasing the particle size [20] this paper adopts the method of generating parts based on the surface first. In this paper, we use the method of generating parts based on the surface and then the Boolean combination of parts to erase the punctured surface of the contact area. Related research [21] shows that the blank section length needs to be greater than or equal to double the pipe diameter, and this length has no effect on the simulation results when it is increased within a certain range, and the container set in this paper is shown in Figure 3.

Figure 3. Vessel and fluid domain

Click the "Automatic Mesh" button under "Geometry-Operation" to complete the meshing operation. In this paper, we choose the cut body mesh, the blank section of the mesh using the default control, the particle accumulation area to establish encrypted surface control, body control, the relevant dimensions are shown in Table 5 (the base size of 0.2m), the generated grid effect is shown in Figure 4.

Table 5. Mesh size setting

Control type	Target surface size	Minimum surface size	Number of prism layers	Total thickness of prismatic layer
Default control	20% Base size	10% Base size	2	5% Base size
Face control	0.002m	0.001m	2	0.002m
Body control	2% Base size		2	1% Base size

Figure 4. Grid effect diagram

3.5 Comparison of simulated and experimental resistance

The comparison of simulated and experimental resistance per unit length is shown in Table6 and Fig.5 to make the comparison more intuitive. it can be seen that the deviation between the two under various conditions does not exceed 5%, which indicates that the validity of the simulation is good and can be used for the subsequent study.

Table 6. Comparison of simulated and experimental resistance results

Wind speed (m/s)	Simulated values (Pa/m)	Experimental value (Pa/m)	Simulation bias (%)
0.035	6.54	6.67	1.92
0.049	10.37	10.00	-3.73
0.060	13.82	13.33	-3.66

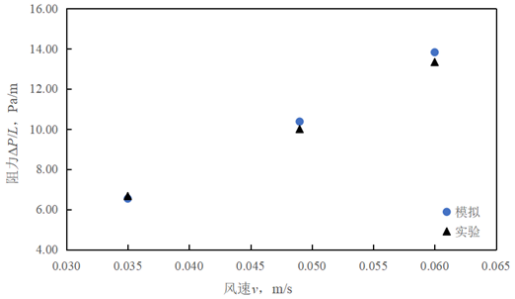

Figure 5. Comparison of simulated and experimental stacked bed resistance at different wind speeds

3.6 Analysis of the effect of particle morphology parameters on the stacking resistance

The particles with diameters of 6mm and 8mm and L/D ratios of 3-6 were used as the research objects to explore the effects of diameter and L/D ratio on the resistance of the stacked bed, and the flow velocities were taken as 0.05m/s. The resistance simulation results are summarized in Figure 6.

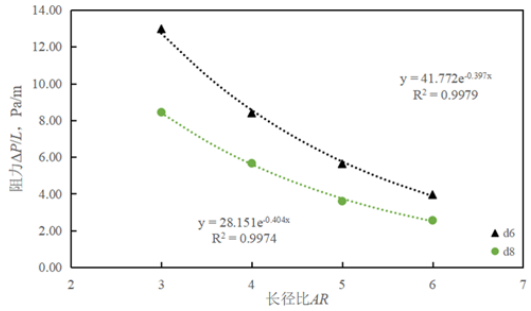

Figure 6. Accumulation bed resistance of particles with different diameters and aspect ratios

Observing Figure 6, it can be found that: when the diameter is certain, the resistance decreases with the increase of L/D ratio, and the R2 fitted with exponential function is higher; when the L/D ratio is the same, the resistance value of stacked bed of particles with larger diameter is always smaller than that of smaller diameter. Therefore, it can be considered that the drag is negatively related to the diameter and negatively related to the L/D ratio.

3.7 Combustion modeling

The furnace model is established and meshed in Workbench as shown in Figure 7. The furnace has a diameter of 200 mm and a height of 300 mm, with an air outlet at the top and 24 circular air inlets of 1 mm diameter arranged in a circular pattern at the bottom.

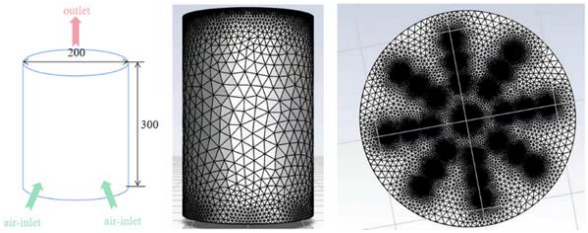

Figure 7. Stove model

3.8 Analysis of the effect of particle morphological parameters on combustion characteristics

In this paper, the combustion efficiency is measured by the percentage of volatile precipitation during the combustion of particles. The particle information can be exported by checking summary in the particle track, and the percentage of volatile emission can be counted; a cloud diagram shown in Figure 8 can be established in the cross section of the furnace center to visualize the volatile emission.

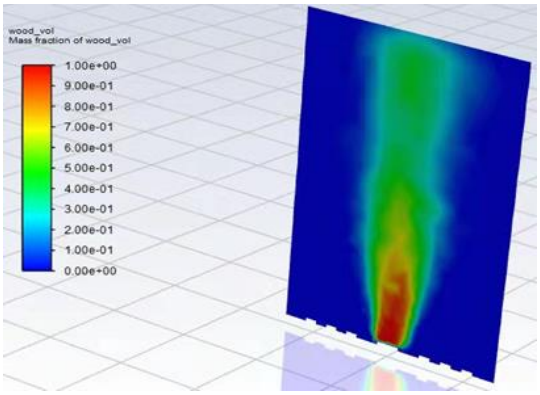

Figure 8. Cloud diagram of volatilization analysis out of the central interface of the stove

By varying the morphological parameters of the particles in the model, the volatilization analysis output ratio was calculated to be between 68% and 82% for 13 particles with different diameters. The variation of the volatile analysis output ratio with particle diameter is plotted in Fig. 9, and it is concluded that the volatile analysis output ratio is low and fluctuates greatly for particles with diameters of 2 mm-7 mm, and high and stable for particles with diameters of 8 mm-14 mm.

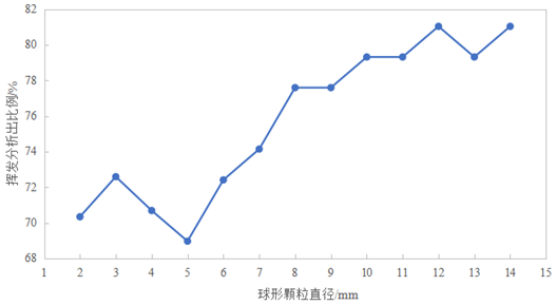

Figure 9. Cloud diagram of volatilization analysis out of the central interface of the stove

4. CONCLUSIONS

(1) A residential house with a typical structure in the northern countryside is used as the design object for load calculation, followed by stove design and establishment of the stove structure, where combustible gas is generated by combustion under the action of primary air, and combustible gas rises and mixes with secondary air for further full combustion.

(2) Comparison of the simulated and experimental resistance per unit length shows that the deviation between the two does not exceed 5% for various operating conditions, indicating that the validity of the simulation is good and can be used for subsequent studies.

(3) Analysis of the effect of particle morphological parameters on the accumulation resistance, the resistance is negatively related to the diameter and negatively related to the aspect ratio. When the diameter is certain, the resistance decreases with the

increase of the L/D ratio, and the resistance value of the stacked bed of particles with large diameter is always smaller than that of small diameter. Therefore, it can be concluded that the resistance is negatively correlated with the diameter and negatively correlated with the L/D ratio.

(4) The combustion efficiency is measured by the percentage of volatilization analyzed during pellet combustion. A cloud diagram was created in the center section of the furnace to visualize the volatilization analysis output. The CFD method was used to investigate the variation of volatile emission ratio with particle diameter, and it was concluded that the volatile emission ratio was low and fluctuating for particles with diameters of 2mm-7mm, and high and stable for particles with diameters of 8mm-14mm.

ACKNOWLEDGMENT

This study was supported by the National Key R&D Program of China No. 2020YFD1100500.

REFERENCE

[1] Hu Y, Xiao BY, Luo WD. Study on the effects of winter heating and coal combustion on indoor air quality in different types of rural dwellings. Modern preventive medicine 1995; (3):180-183.

[2] Ma LY, Dong ZQ, Wu KJ, Pan J. Indoor air quality and fine particulate matter pollution characteristics in rural areas of Guizhou. China Environmental Monitoring 2015; 31(1):28-34.

[3] Pang YX, Jiang DS, Zhang R. Study on the association between long-term indoor coal combustion pollution and carotid atherosclerosis in rural areas. Proceedings of the 2019 National Symposium on Respiratory Toxicology and Health Toxicology.

[4] Wei W. Burning wood and coal for cooking significantly increases heart and lung disease. Family Medicine 2020; 631(03):38-38.

[5] Nemec D, Levec J. Flow through packed bed reactors, Part 1: single-phase flow. Chemical Engineering Science 2005; 60(24):6947-6957.

[6] Macdonald I F，El-Sayed M S ，Mow K， Dullien FAL. Flow through Porous Media-the Ergun Equation Revisited. Ind.eng.chem.fundam 1979; 18(3):199-208.

[7] Park J H, Lee M, Moriyama K, Park HS. Influence of particle morphology on pressure gradients of single-phase air flow in the mono-size non-spherical particle beds. Annals of Nuclear Energy 2018; 115:1-8.

[8] Clavier R, Chikhi N, Fichot F, Quintard, M. Experimental investigation on single-phase pressure losses in nuclear debris beds: Identification of flow regimes and effective diameter. Nuclear Engineering and Design 2015; 292(B4):222-236.

[9] Robert, K, Niven. Physical insight into the Ergun and Wen & Yu equations for fluid flow in packed and fluidised beds. Chemical Engineering Science 2002.

[10] Ozahi E, Gundogdu M Y, Carpinlioglu M. A Modification on Ergun's Correlation for Use in Cylindrical Packed Beds With Non-spherical Particles. Advanced Powder Technology 2008; 19(4):369-381.

[11] Atmakidis T, Kenig E Y. CFD-based analysis of the wall effect on the pressure drop in packed beds with moderate tube/particle diameter ratios in the laminar flow regime. Chemical Engineering Journal 2009; 155(1-2):404-410.

[12] Niksa S. Predicting the macroscopic combustion characteristics of diverse forms of biomass in p. p. firing. Fuel 2021; 283.

[13] Panahi A, Vorobiev N, Schiemann M, Tarakcioglu M， Levendis YA. Combustion details of raw and torrefied biomass fuel particles with individually-observed size, shape and mass. Combustion and Flame 2019; 207:327-341..

[14] Ministry of Housing and Urban-Rural Development of the People's Republic of China. Energy-saving design standards for residential buildings in severe cold and cold regions: JGJ 26-2018. Beijing: China Construction Industry, 2018.

[15] Fan ZS, Zhang Y, Zhang Q. Analysis of energy saving and emission reduction benefits of biomass forming fuel boiler combustion. Applied Energy Technology 2020; 08:39-42.

[16] Liu S C, Jiang J C. Research on the technology of dedicated pellet forming fuel civil stoves. Forestry Chemical Communication 2000; 034(001):10-12.

[17] Shu W. Design and experiment of high efficiency biomass forming fuel cooking stove. Zhengzhou: Henan Agricultural University, 2008.

[18] Xiu, T C. Development and experimental study of biomass forming fuel stoves. Harbin:Harbin Institute of Technology, 2009.

[19] Dixon A G, Nijemeisland M. CFD as a Design Tool for Fixed-Bed Reactors. Industrial & Engineering Chemistry Research 2001; 40(23).

[20] Guardo A, Coussirat M, Larrayoz M A. CFD Flow and Heat Transfer in Nonregular Packings for Fixed Bed Equipment Design. Industrial & Engineering Chemistry Research 2004; 43(22):7049-7056.

[21] Bai H, Theuerkauf J, Gillis P A. A Coupled DEM and CFD Simulation of Flow Field and Pressure Drop in Fixed Bed Reactor with Randomly Packed Catalyst Particles. Industrial & Engineering Chemistry Research 2009.